ISSN (Print) 1226-1750
ISSN (Online) 2233-6656
Journal of Magnetics 25(3), 383-388 (2020) https://doi.org/10.4283/JMAG.2020.25.3.383

Fabrication of Ni/Epoxy Resin Functionally Graded Materials via a Reciprocating Magnetic Field

Jing Li[1,2]* and Xiaoling Peng[2]*

[1]*National Laboratory of Solid State Microstructures, Nanjing University, Nanjing 210093, China*
[2]*College of Material Sciences and Chemistry, China Jiliang University, Hangzhou 310018, China*

(Received 3 October 2019, Received in final form 14 September 2020, Accepted 24 September 2020)

A reciprocating magnetic field was applied to prepare functionally graded materials (FGM) comprised of magnetic Ni and nonmagnetic epoxy resin. The reciprocating field was achieved by shifting a cylindrical permanent magnet along the axis towards or away from the sample in cycle. Ni decreases gradually with the distance from surface to bottom, which attributes to the continuously changing driving force on magnetic Ni particles by the reciprocating field. The gradient of Ni increases with cycle times, while decreases with the increase of the velocity of the reciprocating magnet. The results reveal that it is a more effective way to prepare FGMs by using reciprocating magnetic field compared with normal static magnetic field.

Keywords : functionally graded materials, composites, reciprocating magnetic field, magnetic materials, microstructure

1. Introduction

Functionally graded materials (FGM) are characterized by the variation in composition and structure gradually over volume, resulting in corresponding gradual changes in the properties, which have wide applications in the field of materials science and engineering [1-7]. These materials can be designed for specific functions with a broad range of applications in transportation [8], (bio) mechanical engineering [9], civil or nuclear engineering [10], sensor technology [11], electronics and magnetic devices [12].

The key technique to design and fabricate FGMs is how to vary the microstructure from one material to another material with a specific gradient. The FGMs have been developed by various techniques including powder metallurgy [13], plasma spraying [14], centrifugal casting [15], hot pressing [16], thermo gelation of polysaccharides [17], as well as magnetic field treatment [18]. Previously, Ni/ZrO_2 FGMs have been prepared in a static gradient magnetic field via slip casting in our group [19]. Similarly, Wang *et al.* [20] fabricated MnSb/Sb–MnSb FGMs by a semi-solid forming process under static magnetic field gradients which did not change throughout the experiment. Hu *et al.* [21] prepared aluminum alloy functionally graded material using directional solidification under an axial static magnetic field which did not change either throughout the experiment. Nardi *et al.* [22] fabricated bioinspired functionally graded nanocomposites by employing gradient magnetic field with different driving force. The key aspects of these methods are a distinct difference in magnetic susceptibility of components and a sufficiently steep field gradient, which promise magnetic particles to be pushed to stronger field regions by the magnetic force [19, 20]. The utilization of external magnetic fields provides a promising direction to fabricate FGMs comprising magnetic particles with nonmagnetic matrix. However, the exploration of utilizing external magnetic fields to fabricate FGMs is still less and all researches are currently restricted to static magnetic fields.

In this paper, the FGMs composed of epoxy resin and Ni powders were fabricated with a reciprocating magnetic field. During the preparation process, the sample was exposed to a reciprocating magnetic field caused by the up-and-down motion of a permanent magnet in cycle. Magnetic particles are forced to move towards to stronger field area under the reciprocating magnetic force, which enables to produce the desired composition gradient even in a small magnetic field gradient. The microstructure,

*Co-corresponding author: Tel: +86-571-86875600
Fax: +86-571-86875608, e-mail: jingli@cjlu.edu.cn
Tel: +86-571-86875600, e-mail: pxlqingliu@cjlu.edu.cn.

composition distributions and specific saturation magnetization of Ni/epoxy resin FGMs prepared with the reciprocating field are investigated. The results reveal it is an effective attempt to prepare FGMs.

2. Materials and Methods

Ni powders with a mean diameter of 1.2 μm and epoxy resin (E-51, brand in China) were used as raw materials. Ni is a common component in functionally graded materials. It has good high temperature stability, low coefficient of thermal expansion and excellent magnetic properties, so Ni was chosen in this paper. In this experiment, the Ni content was selected as 5 wt.% and 15 wt.% respectively. Diethylenetriamine was selected as the hardener for curing the epoxy resin. Ni powders and epoxy resin were mixed homogeneously into slurry by mechanical stirring for 1 h. The slurry was then poured into cylindrical mold of 10 × 5 mm in dimensions. The mold was quickly sealed up and laid horizontally right under a cylindrical permanent magnet with the axis of the mold and the magnet coinciding with each other. This is called initial position, where the magnetic field on mold was weak and could be nearly ignored, as illustrated in Fig. 1(a). The magnet was then shifted vertically downward to the mold at a constant velocity by a mechanical device, accompanying with a gradual increase of the field intensity in the mold which was fixed in place. In the experiment, the velocities were selected as 1 mm/s, 5 mm/s, 10 mm/s and 20 mm/s, respectively. Finally, the magnet reached the stop position (Fig. 1(b)), where the magnet and the mold were closed to each other. Then the magnet was moved back to the initial position at the same velocity, during which the field intensity in the mold decrease gradually. This is one cycle. If necessary, the magnet was driven up and down for reciprocating movement for various cycle times (Fig. 1(c)). In the experiment, the cycle times were selected as 2, 5, 10 and 15, respectively. For comparative analysis, some samples were prepared in the stop position (Fig. 1(b)) without the reciprocating movement of magnet. The surface magnetic field strength on the axial centre of the cylindrical magnet is 0.41 T, with a gradient of 2.2 T/m. After the magnetic field was removed, the following curing process was performed at 20 ℃ for 2 h, followed by 0.5 h at 100 ℃.

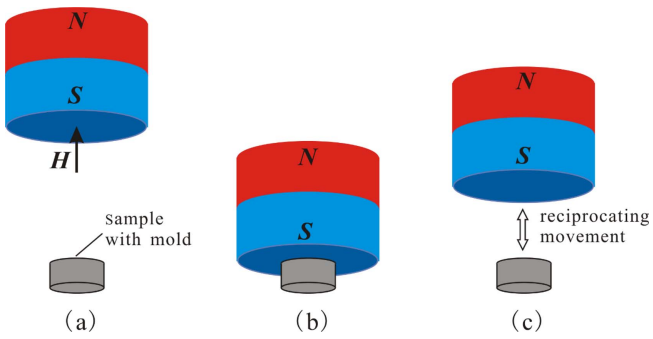

Fig. 1. (Color online) Schematic illustration of sample preparation in a reciprocating magnetic field: (a) initial position; (b) stop position; (c) schematic diagram of reciprocating movement.

The cured 10 × 5 mm cylindrical samples were cut along the axial direction and polished for further characterizations. The longitudinal (parallel to the magnetic field direction) microstructures of the samples were observed by the optical microscopy (MeF-3, Reichert, Austria). The volume distribution of Ni along the axial direction was analyzed by micro-image analysis and process software. The samples were then cut into small pieces for saturation magnetization test, which can reveal the content of magnetic Ni particles more accurately. The magnetic measurement was carried out with a Vibrating Sample Magnetometer (Lakeshore 7407, USA) under a magnetic field range from –2T to 2T.

3. Results and Discussion

Figure 2(a) shows the optical micrographs of the cured sample with reciprocating magnetic field at a velocity of 10 mm/s. The magnet kept on moving until epoxy resin lost the fluidity. As comparation, the optical micrographs of the cured sample under static field at the stop position (Fig. 1(b)) are shown in Fig. 2(b). The contents of Ni for both samples are 15 wt.%. The bright dots dispersed on the black matrix are identified to be Ni. It can be found Ni decreases with the increasing distance from surface to bottom for both samples. It suggests that the gradient distributions are formed under both reciprocating field and static field, which is due to the combination of the field intensity and the field gradient [19]. Ni can be easily magnetized to saturation, and the magnetic force induced on a magnetic particle can be expressed as [23]

$$F \approx \mu_0 V M_S grad H \tag{1}$$

where μ_0 is the magnetic permeability of vacuum, V is the particle volume, M_S is the saturation magnetization, and H is the magnetic field around the magnet. It is this magnetic force that drives Ni redistributed in the slurry.

Apparently, the composition gradient in the sample with reciprocating field is larger than that with static field, which means more Ni particles are driven to the high field area under reciprocating field. In addition, the chain-like Ni clusters are also observed along filed direction in

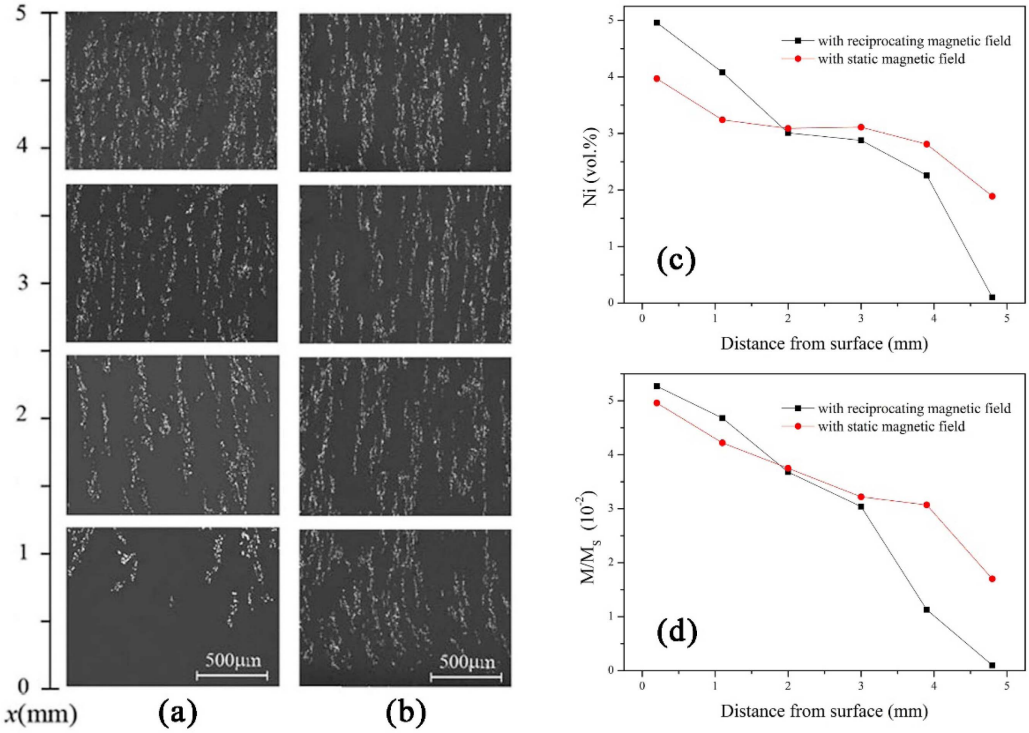

Fig. 2. (Color online) Optical micrographs of cured Ni/epoxy resin FGMs with reciprocating magnetic field (a) and static field (b). Distributions of Ni concentration (c) and specific saturation magnetization (d) as a function of the distance from surface.

both the samples with reciprocating magnetic field and static field, which are attributed to both the magnetic interaction among particles and the field interaction between magnetic field and magnetic Ni particles [24].

The distributions of Ni concentration and specific saturation magnetization on the cross-section of the samples with reciprocating field and static field are plots in Figs. 2(c) and 2(d), respectively. All samples consist of magnetic Ni and nonmagnetic epoxy resin, so the specific saturation magnetization can exactly represent the volume content of Ni. Both Ni concentration and specific saturation magnetization decrease with the increase of distance from surface to bottom. The gradients of Ni concentration of the sample with reciprocating field are larger than that with static field. It indicates that it is more effective to prepare FGMs in this reciprocating magnetic field than that in static field.

It is very surprising and interesting that the composition gradient in the sample with reciprocating field is larger than that with static field, because the field intensity and field gradient on the mold become strong and weak alternately for the reciprocating field, while they are always large for the static field. It is probably attributed to the alternating effect of reciprocating field on samples. Once Ni particle moves at a velocity through the slurry, which can be regarded as a viscous liquid, it would experience viscous force [25]. When a magnetic field is applied to the suspension containing magnetic particles, its viscosity increases rapidly with the increase of the field strength, especially for concentrated suspension. The increasing viscosity makes magnetic Ni move difficultly in the slurry. In the static field, Ni particles will stop moving if the magnetic driving force is not sufficient to overcome the resistance. While in the reciprocating field, the magnetic driving force, the resistance, the viscosity, and the positions of neighboring particles are changing with the time. At one moment, one Ni particle may be blocked due to the resistance. At the next moment, the situation may have changed. Under reciprocating field, the nearby particles that once hindered the movement of Ni may move away because the viscosity may become lower and the resistance may become less, so the Ni particles can start to move again. Finally, more magnetic Ni particles can move to the high field area, and large composition gradient is formed in reciprocating field.

Figures 3(a)-3(d) show the optical micrographs of the samples with reciprocating field at the velocity of 1 mm/s, 5 mm/s, 10 mm/s and 20 mm/s, respectively. The magnet cycled 10 times on the samples with 5 wt.% Ni. It is obvious that Ni decreases gradually from surface to bottom in all samples with different velocities. The composition gradient of the sample with low velocity

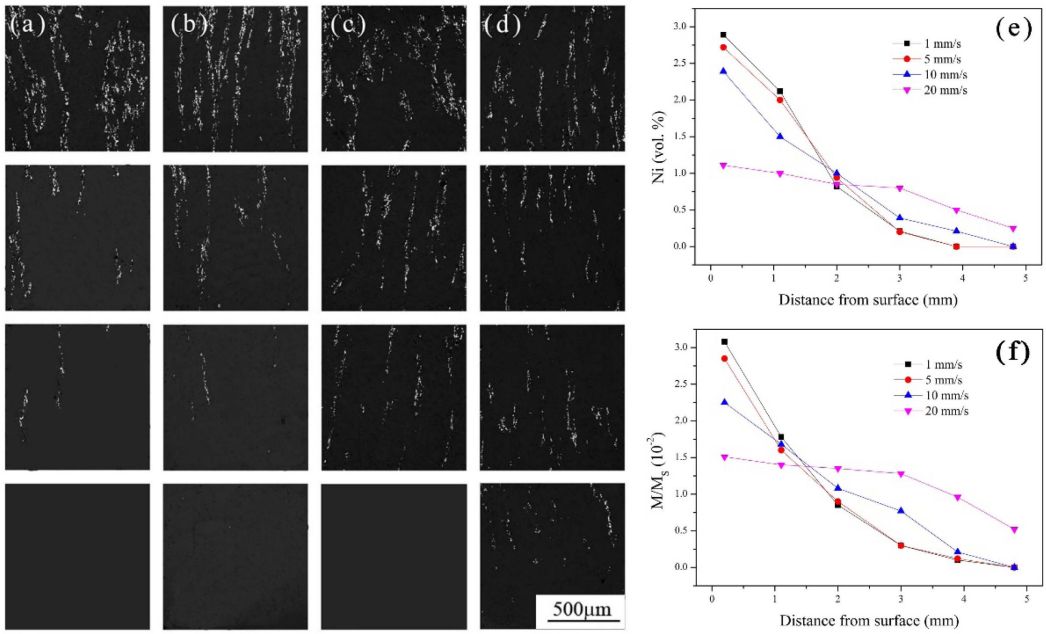

Fig. 3. Optical micrographs of Ni/epoxy resin FGMs with various velocities: (a) 1 mm/s; (b) 5 mm/s; (c) 10 mm/s; (d) 20 mm/s. Distributions of Ni concentration (e) and specific saturation magnetization (f) with various velocities as a function of the distance from surface.

seems larger than that with high velocity. Figures 3(e) and 3(f) plot the distributions of Ni concentration and specific saturation magnetization at the cross-section of the samples with various velocities. The results show that the composition gradient decreases with the increase of velocity, and the slower velocity results in larger gradient.

Each Ni particle in slurry under magnetic field would experience viscous force. The value of viscous force is determined by Stokes' law [25], which is proportional to velocity of the Ni particle. The viscous force hinders the free moving of Ni particle, which makes Ni cannot always follow the movement of magnet, especially at a

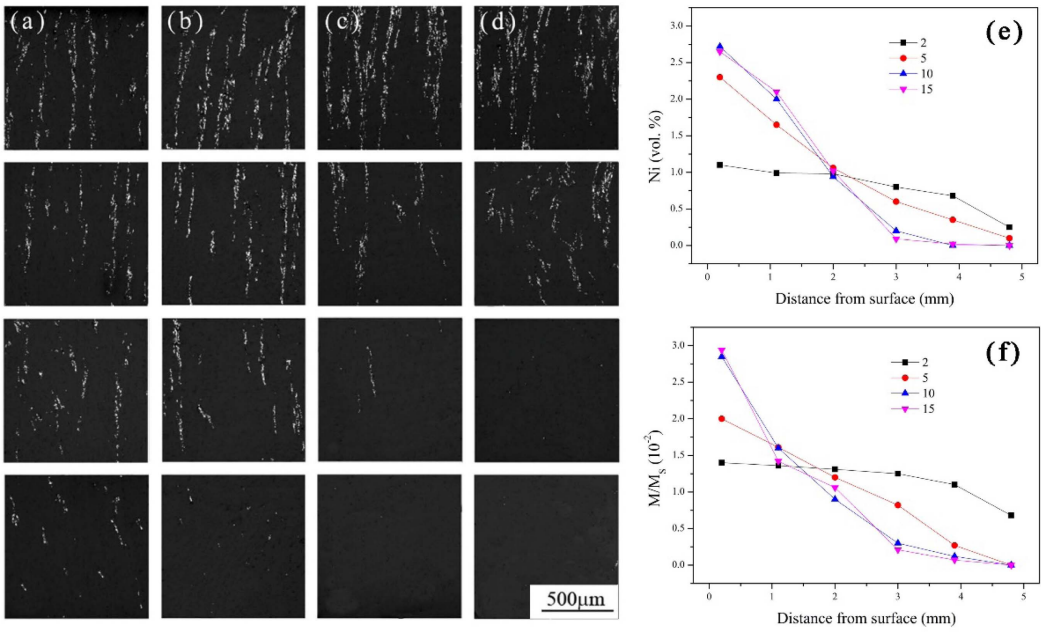

Fig. 4. Optical micrographs of Ni/epoxy resin FGMs with various cycle times: (a) 2; (b) 5; (c) 10; (d) 15. Distributions of Ni concentration (e) and specific saturation magnetization (f) with various cycle times as a function of the distance from surface.

relative high velocity. It suggests the reciprocating magnetic field with slow velocity drives more magnetic particles to high field area. In addition, the low velocity means the effect of magnet field applied on Ni particle lasts for a long time, which also leads to a steeper composition gradient.

Figures 4(a)-4(d) show the optical micrographs of the samples with reciprocating field with the cycle times of 2, 5, 10 and 15, respectively. The velocity of the magnet was 5 mm/s. The content of Ni was 5 wt.%. It can be found that Ni distributions decrease gradually from surface to bottom for all samples with different cycle times. The composition gradient increases with cycle time. Figures 4(e) and 4(f) plot the distributions of Ni concentration and specific saturation magnetization at the cross-section of the samples with various cycle times. The results show that the gradient of Ni increases with cycle time, and when the reciprocating field cycles increase to more than 10 times, the composition gradient keeps nearly unchanged.

As discussed above, the moving of Ni particle is hindered by viscous force, and Ni always moves behind the magnetic field. It is impossible to make Ni moves fluently following the magnetic field at one single cycle. More cycles make more Ni particles move to the top area following the field, and thus form a larger gradient. Once most of magnetic particles are moved to the top region, the magnetic interaction among particles increases rapidly and the more stable and larger clusters are formed. Therefore, the composition distribution remains stable after certain cycles.

Moreover, there are similar distributions for Ni concentration (Figs. 2(c), 3(e) and 4(e)) and specific saturation magnetization (Figs. 2(d), 3(f) and 4(f)), but some differences in numerical values. The distribution curves of Ni concentration are calculated from the optical micrographs on the cross-section. The calculated values have some differences with the actual volume fraction of Ni, because Ni distributes spatially unevenly at the same distance from surface. Therefore, the distribution of specific saturation magnetization of the samples represents the volume content of Ni more exactly.

4. Conclusions

In this work, a novel and facile method is developed to fabricate Ni/epoxy resin FGMs with a reciprocating magnetic field which drives the Ni particles to move in the slurry. The gradient of the samples increases with cycle times, while decreases with the increase of velocity of reciprocating magnet. Compared to the preparation of FGMs by using static magnetic field, the fabrication of FGMs in reciprocating field is more effective and attractive, which is very promising in scientific and technological applications.

Acknowledgments

This work was supported by Public Projects of Zhejiang Province (LGG19E010002), Natural Science Foundation of Zhejiang Province (LY16E030004), National Natural Science Foundation of China (No. 51002132, 51402276), State Key Laboratory of Silicon Materials (SKL2016-11) and China Postdoctoral Science Foundation (2014M561615).

References

[1] L. D. Bobbio, R. A. Otis, J. P. Borgonia, R. P. Dillon, A. A. Shapiro, Z. K. Liu, and A. M. Beese, Acta Materialia **127**, 133 (2017).
[2] S. Zhao, S. J. Li, S. G. Wang, W. T. Hou, Y. Li, L. C. Zhang, Y. L. Hao, R. Yang, R. D. K. Misra, and L. E. Murr, Acta Materialia **150**, 1 (2018).
[3] B. E. Carroll, R. A. Otis, J. P. Borgonia, J. O. Suh, R. P. Dillon, A. A. Shapiro, D. C. Hofmann, Z. K. Liu, and A. M. Beese, Acta Materialia **108**, 46 (2016).
[4] I. Gotman and E. Y. Gutmanas, Advanced Engineering Materials 20 (2018).
[5] B. Saleh, J. Jiang, R. Fathi, T. Al-hababi, and A. Ma, Compos. Part B Eng. 201 (2020).
[6] R. Fathi, A. Ma, B. Saleh, Q. Xu and J. Jiang, Mater. Today Commun. 24 (2020).
[7] I. M. El-Galy, B. I. Saleh and M. H. Ahmed, SN Appl. Sci. 1 (2019).
[8] G. Y. Sun, G. Y. Li, S. J. Hou, S. W. Zhou, W. Li, and Q. Li, Materials Science And Engineering a-Structural Materials Properties Microstructure And Processing **527**, 1911 (2010).
[9] Q. L. Meng, Y. N. Liu, H. Yang, and T. H. Nam, Scripta Materialia **65**, 1109 (2011).
[10] H. L. Dai, Y. N. Rao, and T. Dai, Composite Structures **152**, 199 (2016).
[11] T. J. Hu, X. D. Li, Y. H. Li, H. Wang, and J. Wang, Materials Letters **65**, 2562 (2011).
[12] F. Ebrahimi and M. R. Barati, Smart Materials And Structures 25 (2016).
[13] X. Jin, L. Z. Wu, Y. G. Sun, and L. C. Guo, Materials Science And Engineering a-Structural Materials Properties Microstructure And Processing **509**, 63 (2009).
[14] Siddhartha, A. Patnaik, and A. D. Bhatt, Materials & Design **32**, 615 (2011).
[15] J. Y. Kim, V. Adinolfi, B. R. Sutherland, O. Voznyy, S. J. Kwon, T. W. Kim, J. Kim, H. Ihee, K. Kemp, M. Adachi, M. J. Yuan, I. Kramer, D. Zhitomirsky, S. Hoogland, and E. H. Sargent, Nature Communications 6 (2015).
[16] G. Miranda, A. Araujo, F. Bartolomeu, M. Buciumeanu,

O. Carvalho, J. C. M. Souza, F. S. Silva, and B. Henriques, Materials & Design **108**, 488 (2016).
[17] M. C. Tanzi, S. Bozzini, G. Candiani, A. Cigada, L. De Nardo, S. Fare, F. Ganazzoli, D. Gastaldi, M. Levi, P. Metrangolo, F. Migliavacca, R. Osellame, P. Petrini, G. Raffaini, G. Resnati, P. Vena, S. Vesentini, and P. Zunino, J. Appl. Biomater. Biom. **9**, 87 (2011).
[18] M. Dong, T. Liu, J. Liao, Y. B. Xiao, Y. Yuan, and Q. Wang, J. Alloys Compd. **689**, 1020 (2016).
[19] X. Peng, M. Yan, and W. Shi, Scripta Materialia **56**, 907 (2007).
[20] T. Liu, Q. Wang, A. Gao, C. Zhang, C. J. Wang, and J. He, Scripta Materialia **57**, 992 (2007).
[21] S. D. Hu, A. Gagnoud, Y. Fautrelle, R. Moreau, and X. Li, Sci. Rep. 8 (2018).
[22] T. Nardi, Y. Leterrier, A. Karimi, and J. A. E. Manson, Rsc Advances **4**, 7246 (2014).
[23] I. Mălăescu, L. Gabor, F. Claici, N. Ştefu, J. Magn. Magn. Mater. 222 (2000).
[24] M. Yan, X. L. Peng, and T. Y. Ma, J. Alloys Compd. **479**, 750 (2009).
[25] T. Manik and B. Holmedal, Acta Materialia **61**, 653 (2013).